Plasma Sources Sci. Technol. **9** (2000) 87–96. Printed in the UK PII: S0963-0252(00)11053-9

Damped dust oscillations as a plasma sheath diagnostic

E B Tomme†, B M Annaratone and J E Allen

Department of Engineering Science, University of Oxford, Parks Road, Oxford OX1 3PJ, UK

E-mail: ed.tomme@usafa.af.mil, beatrice.annaratone@eng.ox.ac.uk and john.allen@eng.ox.ac.uk

Received 10 August 1999, in final form 17 November 1999

Abstract. Dust can be suspended in a plasma sheath under certain conditions. An analysis of the dust trajectory as it approaches its equilibrium suspension height can provide a description of the spatial variation of the potential in the sheath. We describe an experiment in which we track such trajectories and calculate their oscillation frequencies, equilibrium heights and damping constants. These three measured parameters are then interpreted in such a manner as to reveal the neutral drag force on the dust and the curvature of the sheath electric potential in which the dust moves. We then calculate the charge on the dust particles suspended in the plasma sheath. We also show that, to a high degree of accuracy, the sheath potential predicted by several numerical models in the literature as well as by our experimental results is parabolic, i.e. the sheath field is quite linear.

1. Introduction

The understanding of dust in a plasma sheath is of great importance to researchers in a variety of disciplines. The study of dust levitating in terrestrial sheaths, especially in so-called plasma crystals, has been underway since 1994, when Chu *et al* [1] and Thomas *et al* [2] experimentally produced such crystals. One of the properties of such dust that is not well understood, either experimentally or theoretically, is its charge.

The analysis of the trajectories of dust particles oscillating in a plasma sheath has been used as a method for determining the charge on the dust by a number of researchers during the past few years. Groups in Germany first used a time varying potential [3–5] induced across the sheath and, more recently, a laser [6] to cause resonant oscillation of dust in a plasma crystal. Harmonic resonance equations were then used to determine the dust charge. Nunomura *et al* [7] used an observed natural instability in the dust position to calculate the dust charge. However, many of these experiments rely upon assumptions about the nature of the plasma sheath potential or the charging of dust in such a potential, significantly perturb the sheath during the experiment, discount the effects of significant forces in the system, or involve some combination of the above. The specific effects of these assumptions and techniques will be discussed later in this paper. Konopka *et al* [8] and Morfill *et al* [9] have also used horizontal collisions of dust particle pairs to determine the interaction potential of the collision, and from that potential, the charge on the dust. Their self-consistent method does not require any external assumptions concerning plasma parameters or charging mechanisms, but their reported error is larger than the other techniques. In this paper, we present a novel [10] use of the dust oscillation technique that highlights (and stays within) the limits of the assumptions noted above while maintaining stable experimental conditions and accounting for every significant force.

Small particles present in plasmas tend to acquire a negative charge due to the higher mobility of electrons in the plasma. In terrestrial plasmas, negatively charged particles of sufficient size fall toward lower regions of the plasma until they reach the plasma sheath. In the sheath, the electric field from the negatively self-biased electrode begins to repel the particles, or dust. Under certain conditions, this repulsion is sufficient to cause the dust to suspend above the lower electrode. At this point, the particles encounter a balance between upward and downward forces, or in other words, they encounter a minimum in the potential well formed by the sum of these forces.

As a dust particle falls from the plasma into the sheath and enters the potential well, its trajectory oscillates about an equilibrium height, the damping of the oscillations being related to the chamber pressure and the dust mass. An initial analysis of several trajectories indicated that the oscillations might be approximately damped harmonic.

In order to explain this motion, we will first present a review of applicable damped harmonic motion theory. Next, we will develop a theory that uses dust trajectory parameters to estimate the charge on a dust particle at its equilibrium height. We will then discuss a simple model of a collisional radio frequency (RF) plasma sheath needed for our charge estimation theory. Finally, we will present experimental

† Permanent address: Department of Physics, United States Air Force Academy, Colorado 80840, USA.

 © 2000 IOP Publishing Ltd

results of our trajectory analysis for a number of dust particles with different masses at different pressures.

2. Harmonic dust oscillation theory

As previously stated, dust in a plasma sheath oscillates in a potential well formed by the opposing electrostatic and gravitational forces. While those forces are not the only forces acting on the dust (ion drag being the most significant of the other forces), they have been shown to be several orders of magnitude larger than other dust-velocity-independent forces in the upper sheath region where our experimental data were taken for most of the studied particle sizes [11–13]. For the smaller particles (<2.5 μm radius), the ion drag begins to approach the magnitude of the gravitational force. However, we will show that the change on the calculated dust charge due to consideration of this force for these smaller particles will be less than the error of our technique. For this reason, we will ignore dust-velocity-independent forces other than gravity and electrostatic repulsion.

Our initial hypothesis was to test whether the oscillations were harmonic, and if so, over what amplitude range. To test this theory, we fit our data to the well known equation of motion for the damped harmonic oscillator, for example [14],

$$m\ddot{z} + \gamma\dot{z} + \kappa(z - z_{eq}) = 0 \tag{1}$$

where m is the particle mass, γ is the drag constant, κ is the restoring constant, z is the particle height above the electrode (the subscript 'eq' denotes the equilibrium height), and $\dot{z}$ and $\ddot{z}$ are the first and second time derivatives of the height.

For an undamped oscillator with a restoring force $F(z) = -\kappa z$ the potential well has the form $U(z) = \frac{1}{2}\kappa z^2$, showing that the curvature of the potential is just $\kappa/2$. By adding the damping term, we do not change the shape of the well; we merely allow energy to leave the system. It can be shown that for the damped simple harmonic oscillator,

$$\kappa = m[(2\tau)^{-2} + \omega^2] \tag{2}$$

where the damping time constant, τ, is defined by

$$\tau = \frac{m}{\gamma}. \tag{3}$$

Equation (2) demonstrates that the curvature of the potential well may be found by measuring the damping time constant and the oscillation frequency.

Measurements of the oscillation parameters described above not only yield data on the potential well, but also can be directly compared with the standard drag theory of Epstein [15]. Other researchers [6] have previously shown that this drag law holds in the plasma sheath. Should the data confirm that our dust particles follow the Epstein law, it will provide an additional, independent check on the plausibility of our measured values.

3. Dust charge theory

The charge on dust particles suspended in the plasma is not well known. Recent experimental and theoretical estimates

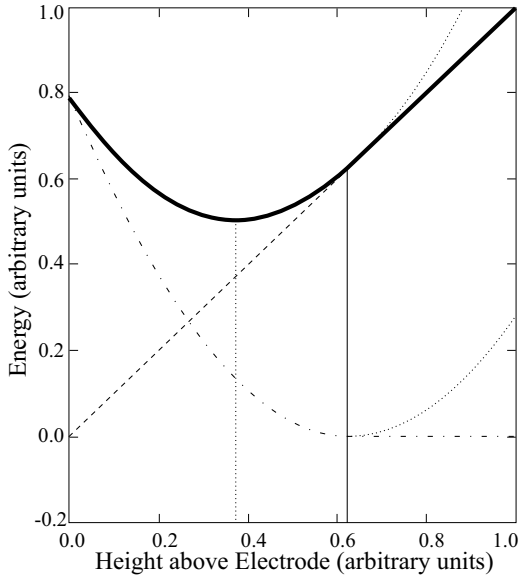

Figure 1. The theoretical potential well. This schematic diagram shows how a harmonic total potential results from the addition of the linear gravitational potential and a harmonic electric potential energy curve. The location of the sheath edge is shown by the vertical full line and the dust equilibrium height is indicated by the vertical dotted line. In this model, the electric potential (dash-dot curve) is essentially zero to the right of the sheath edge. This causes the total potential (full curve) to be parabolic in the sheath and linear in the plasma. The gravitational potential is shown as a dashed line. The dotted extensions to the total and electric potential energy curves show their full parabolic forms. Note that in this figure, the electric potential energy is zero at the minimum point of the parabola, while later in this paper we define zero electric potential at the sheath edge.

place its value on the order of roughly 10^3–10^4 electron charge units for micrometre-sized particles in plasmas with pressures on the order of 10 Pa and electron densities on the order of 10^{16} m^{-3} [3, 5, 6, 16]. The value of about 4000 electron charges on a 4.7 μm radius particle from [4] is the only published value directly comparable with results presented in this paper (melamine formaldehyde dust suspended in an argon plasma sheath), although that value was quoted for dust in a plasma crystal suspended in a perturbed sheath. As we will show here, analysis of the damped oscillation of a dust particle can provide another method to estimate this value.

The total potential in which the dust moves in the sheath is formed by the sum of the electrical and gravitational potential energies,

$$U_{tot} = U_e + U_g \tag{4}$$

as shown in figure 1. The gravitational potential energy is simply $U_g = mgz$, where g is the gravitational acceleration. The determination of κ, as discussed above, fixes the curvature of the total potential energy for small-amplitude oscillations, and the position of its minimum is fixed by the measurement of the equilibrium height, z_{eq}.

Determination of the electric potential energy is not as straightforward. Our assumption of a parabolic total potential and the linear gravitational potential implies that the electric

potential must also be parabolic. Transforming the line-plus-parabola form of the electric potential energy

$$U_e(z) = \left(\frac{\kappa}{2}(z - z_{eq})^2 + U_{eq}\right) - mgz \tag{5}$$

into the standard form ($y = K(z - z_0)^2 + y_0$)

$$U_e(z) = \frac{\kappa}{2}\left[z - \left(z_{eq} + \frac{mg}{\kappa}\right)\right]^2 + \left(U_{eq} - \frac{(mg)^2}{2\kappa} - mgz_{eq}\right) \tag{6}$$

allows us to identify the distance from the electrode at which the extremum occurs. This distance

$$z_0 = z_{eq} + \frac{mg}{\kappa} \tag{7}$$

is a rough gauge of the sheath thickness predicted by this harmonic theory, assuming now that the electric potential is globally harmonic throughout the sheath. As the curvature of this parabola, $\kappa/2$, is the curvature of the *electric potential energy*, we cannot draw any direct conclusions about the magnitude of the curvature of the *electric potential* without knowing the charge on the dust; all we have assumed is that both the potential and the potential energy are harmonic.

At this point, these harmonic assumptions and conclusions may seem quite tenuous. Other researchers [3, 5, 6] have used similar assumptions *a priori*; we will use them here and later justify their use by showing that our data and the results from models available in the literature independently support the parabolic assumptions. In fact, we will show that the data and models support the parabolic assumptions *globally* in the sheath.

The electric potential energy of a dust particle is just

$$U_e(z) = Q_d V(z) \tag{8}$$

where Q_d is the charge on the dust and $V(z)$ is the electric potential. It can readily be shown that physically, κ represents $-Q_d(\mathrm{d}^2V/\mathrm{d}z^2)$ or, equivalently, $Q_d(\mathrm{d}E/\mathrm{d}z)$, where E is the electric field.

By assuming a parabolic sheath total potential energy and a constant dust charge throughout the oscillation, we obtain the charge on the dust at its equilibrium height

$$Q_d = \frac{(mg)^2}{2\kappa\left(V(z_{eq}) - V_0\right)} \tag{9}$$

where V_0 is the extreme value of the (harmonic) electric potential. In equation (9), m and κ are experimentally determined parameters. The potential difference in that equation, however, is not experimentally determinable by current probe methods. To fix its value, we need to rely on a model of the sheath.

4. A simple parabolic sheath model

We are currently in the process of developing an improved numerical model of the RF plasma sheath that is valid for wide ranges of the collisionality parameter (the ratio of the Debye length to the ion mean free path at the sheath edge). This model will also incorporate velocity-dependent ion collision cross sections. We expect to publish this model in the near future. During the course of the development of this model, we have conducted detailed analyses of a number of other models from the literature [17–20]. We determined that one thing all the models have in common is that a simple parabola is an extremely good approximation for the form of the time-averaged electric potential over the entire spatial extent of the sheath.

To construct such a parabolic approximation, one merely needs to know the RF self-bias potential at the electrode and the potential and field at the sheath edge. For the plasma parameters involved in our experiment, we needed to use a collisional model that was valid for the collisionality parameter, α, greater than unity, where $\alpha = \lambda_D/\lambda$, λ_D is the electron Debye length and λ is the ion mean free path. In this model, we assume cold ions so that the diffusion term in the ion transport equation is much less than the mobility term. The ions are then assumed to reach terminal velocity between collisions such that the collisional force equals the electric force at any point in the plasma [20]. This may be expressed as $Mv_i v_i = eE$, where M is the ion mass, v_i is the ion–neutral collision frequency, e is the elementary charge and v_i is the ion velocity. As $v_i = v_i/\lambda$, the electric field at any point in the plasma is $E = Mv_i^2/e\lambda$. The ions reach the Bohm speed at the sheath edge [21], where $v_B = (kT_e/M)^{1/2}$ and kT_e is the electron temperature in energy units. Thus, the electric field at the sheath edge in the modelled plasma is just

$$E_s = kT_e/e\lambda. \tag{10}$$

(This field is also the limiting value of the sheath-edge field for marginally-collisional plasmas proposed by Riemann [22], $E_s = kT_e/e\lambda_D^{2/5}\lambda^{3/5}$, in the limit $\alpha \to 1$.)

Using this field at the sheath edge, our parabolic approximation differs from several accepted models [17, 19, 20], as well as from our own developmental model, by no more than 1% across the entire sheath for parameters similar to our experimental conditions. We thus consider the harmonic nature of the potential in the sheath to be a general result. The parabolic approximation and the Blank model [17] for a set of specific plasma parameters are shown in figure 2 to illustrate the quality of the approximation.

5. Experimental procedure

The well-like nature of the total sheath potential became quite apparent while we were performing experiments that involved observation of dust dropped through the plasma. The experimental set-up is shown in figure 3. It is similar to that used by most other dust oscillation researchers. The 23 cm diameter vacuum chamber is 13 cm high and, for this experiment, the electrodes had diameters of 18 cm and were set 4 cm apart. The upper electrode was grounded and the lower driven by a matched 13.56 MHz RF voltage source. It must be noted that for the plasma parameters used in these experiments, this electrode configuration resulted in an asymmetric situation. The plasma was not only strongly influenced by the potentials on the electrodes, but by the grounded chamber as well, which made the effective size of the driven electrode smaller. This asymmetry resulted in a

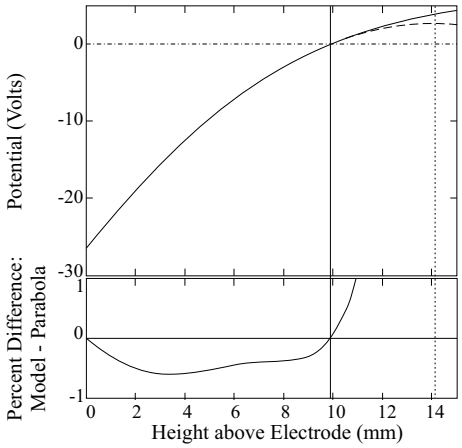

Figure 2. Parabolic fit to the average potential. The upper frame shows a typical numerical potential from the model of Blank [17] (full curve) and the parabola fit to the boundary conditions described in the text (dashed curve). The horizontal dash-dotted line shows the sheath potential (while Blank does not explicitly identify this potential as the sheath potential, our analysis shows that it occurs approximately at the point where the field equals that given by equation (10)). The vertical full line is the sheath edge derived from the numerical data and the vertical dotted line is the harmonic theory sheath edge derived in equation (7). The numerical and harmonic potential curves are indistinguishable at this scale until just above the numerical sheath edge, where the divergence becomes more pronounced. The lower frame shows the difference between the numerical data and the parabolic fit, demonstrating the close approximation harmonic theory makes to the numerical results.

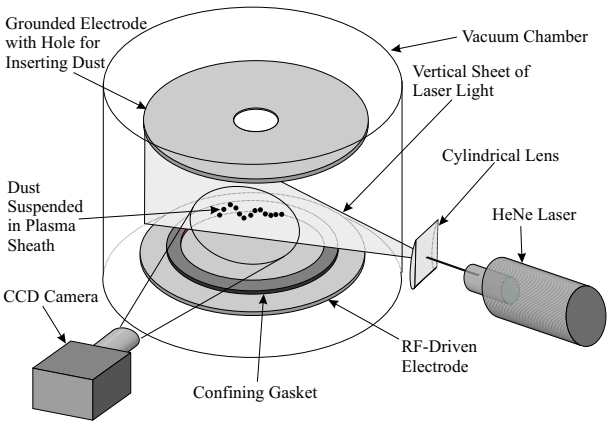

Figure 3. Experimental set-up. The set-up is described in detail in the text.

large fraction of the RF potential appearing across the driven sheath [23].

The dust used in our experiments was spherical melamine formaldehyde ($\rho = 1510$ kg m^{-3}), an insulating polymer, of a variety of individual sizes ranging between approximately 0.5 and 7 μm in radius. The spheres were quite monodispersive, having a quoted radius variation of less than about 0.1%. Prior to each trial, a specific size dust was loaded into a glass container suspended above the upper electrode (not shown in the figure). Very small numbers of dust particles (<10) were dropped through the hole in the upper electrode into the plasma. As it entered the plasma, the dust was illuminated by a HeNe laser beam that had been spread to a thin, vertical sheet. A small, rectangular copper gasket ($2.5 \times 10 \times 0.2$ cm, with a 0.5×8 cm slit removed from its centre) was placed on the lower electrode to form a small potential well that localized the dust in the central region of the chamber. The high aspect ratio of the slit confined the dust to the region illuminated with the laser, but allowed the dust to spread out along the laser beam, minimizing the effects of forces between particles. A high-speed (up to 12 000 fps), image-intensifying CCD camera was employed to record the dust trajectories. Dust trajectories were monitored via the CCD display and recorded digitally directly to a computer.

Dust trajectories were analysed by identifying a particle that underwent a number of oscillations with only minor interaction with its neighbours. Once a particle was identified, its position was manually tracked over a number of frames ($\sim$100). The position and position error data was then corrected for scale, perspective, and gasket perturbation, and a plot of the height-above-electrode against time was then generated.

Our experimental technique differs from previously cited dust oscillation techniques [3–9] in several respects. Those methods typically use some induced or natural driving force to cause resonant oscillation. Our technique is much simpler, although its accuracy for very low-mass particles diminishes due to the very high damping rate for these conditions.

We did not vary the self-bias of the driven electrode nor did we place any variable-bias external probes near the dust. This allowed us to base our results on a stable sheath with a potential profile that is essentially time-independent on the scale of the relevant dust charging times. We also did not have to account for the non-zero electrode currents that would have naturally flowed during induced, slow oscillations of the self-bias. Thus, our method does not involve any external sheath perturbations, the effects of which would tend to greatly complicate any charge analysis.

The benefit of the resonant analysis used in other techniques would seem to be quite apparent, especially for low-mass particles and/or high pressures where the damping is so high that very few oscillations may be observed by our undriven method. This would seem to be especially true for relatively non-intrusive methods that utilize lasers to excite the resonance without disturbing the sheath. However, with all of these resonant methods, there exists the possibility of inadvertently overdriving the resonant oscillations to the point where charge fluctuations on the dust particle become significant enough to spoil the harmonic nature of the potential well. (For a discussion of this charge fluctuation, see e.g. [7, 19, 24, 25].) For small-amplitude oscillations, our results will show the oscillations to be extremely well modelled by harmonic equations, implying that the charge fluctuations are either very small or average out during the oscillation. However, as the oscillation amplitude increases past a critical point, the harmonic nature of the potential breaks down rapidly, invalidating techniques that rely on harmonic equations to obtain charge from the now-anharmonic resonance frequency. We have found this critical amplitude to be typically about 10–20% of the sheath width, based on results presented later in this paper. At the sampling rates used in several of the cited experiments, it would appear to be difficult to determine whether the oscillations were indeed harmonic or merely periodic.

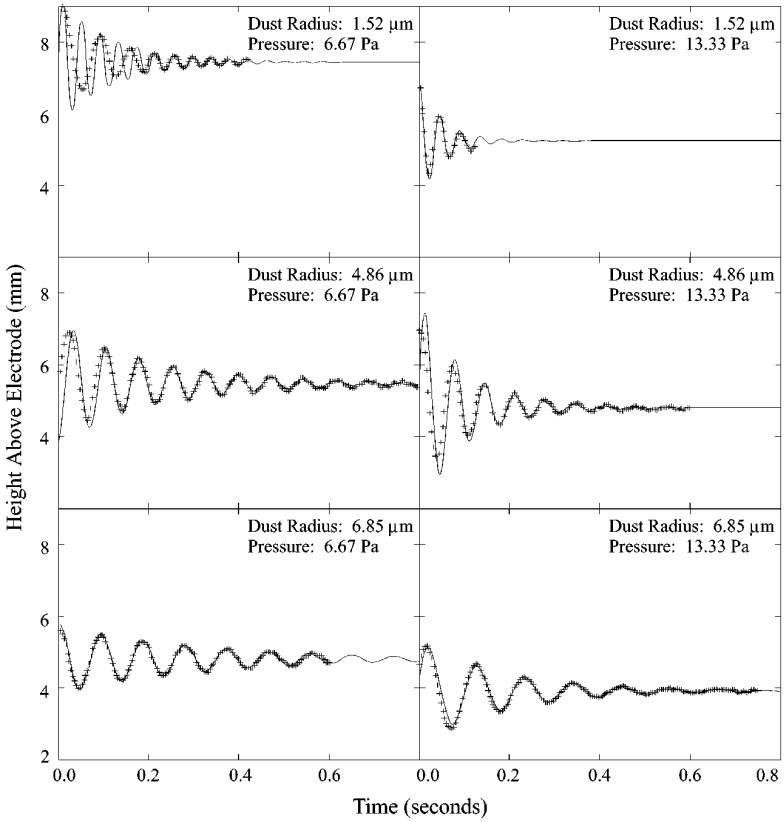

Figure 4. Dust oscillation data and harmonic theory. These six plots show dust trajectories obtained as described in the text. The scales and origins are the same for all six plots to facilitate direct comparison. The full lines are damped harmonic theoretical curves from equation (11) using the parameters shown in table 1. Typical position errors are on the order of 10 μm; these error bars are not visible at this scale. Each column of plots is for the same pressure, while each row of plots is for the same mass dust particle. The other experimental parameters are discussed in the text.

We also go to great lengths to eliminate extraneous forces acting on the oscillating dust. Several of the cited techniques involve the resonant excitation of dust in a crystal lattice, and then use harmonic equations to find the charge on the excited dust. This analysis fails to take into account the strong interaction potentials between the large numbers of dust particles in the lattice, leading to questionable results. Our analysis involves very small numbers of particles inserted into the sheath, and only particles that are observed to be relatively free of interaction with other particles are used for our charge analysis.

We also measured oscillations that occur in the vertical plane. Techniques that utilize horizontal oscillations generally only determine the shape of the confining potential well of the gasket and the interaction potential between dust particles. While these techniques can derive a value for the dust charge, they give little information on the vertical potential profile through significant fractions of the sheath.

Some previous techniques have also relied upon estimates of the charged particle densities from such sources as extrapolations of sine-shaped ion density profiles into the sheath, assumptions that the sheath is a perfect rectifier, or Child–Langmuir ion profiles. Our method instead uses the previously discussed assumption of a harmonic sheath potential.

6. Experimental results

The solution to the equation of motion (equation (1)) is

$$z(t) = \exp\left(-\frac{t}{2\tau}\right)\left[z(0)\cos(\omega t) + \frac{\dot{z}(0) + (z(0)/2\tau)}{\omega}\sin(\omega t)\right] + z_{eq} \qquad (11)$$

where t is the time and ω is the observed oscillation frequency. Thus, our curve-fitting routine used the five parameters $z(0)$, $\dot{z}(0)$, z_{eq}, ω, and $(2\tau)^{-1}$ to fit the damped harmonic theory (equation (11)) to our data. Table 1 lists the plasma and relevant curve-fitting parameters for all the data sets. Six typical plots of our experimental data and the associated curve fits from the damped harmonic theory are shown in figure 4. The plots show combinations of three different radii dust particles taken at two different pressures. The decrease in the equilibrium height with an increase in pressure and/or mass is apparent, as is the decrease in the damping rate as the pressure is decreased and/or the mass is increased. The difference in oscillation frequency between the small and large particles is also visually apparent.

In many of the trajectories, the average error between the data points and the theoretical fit over a large portion of the plot is less than the width of a pixel (1 pixel $\cong$ 30 μm) from a data image frame. We also emphasise that the theoretical fit to the data is very good for oscillations that approach

Table 1. Experimental conditions and curve-fitting parameters. The data in the first two columns are the controlled experimental conditions. The data in the central three columns are the resulting curve-fitting parameters (errors for oscillation frequencies and decay constants are estimated). The data in the last four columns are derived from data in the other columns using the equations indicated. For all cases the electrode spacing was 40.0 mm, the RF amplitude was 96.4 V, the RF frequency was 13.56 MHz, the dust density was 1510 kg m^{-3}, and the working gas was argon. For the high-pressure case, kT_e and n_0 were 3.9 eV and 2.4×10^{15} m^{-3}, respectively, while at low pressure they were 3.7 eV and 1.7×10^{15} m^{-3}. The plasma parameters were determined by Langmuir probe measurements at the centre of the plasma. The visually-determined sheath widths were 9.4 ± 0.25 mm and 8.5 ± 0.25 mm for 6.67 Pa and 13.33 Pa, respectively.

Dust radius A (μm)	Chamber pressure P (Pa)	Equilibrium height z_{eq} (mm)	Oscillation frequency ω (rad s^{-1})	Decay constant $(2\tau)^{-1}$ (s^{-1})	Dust mass $4\pi r^3\rho/3$ (10^{-13} kg)	Restoring constant, equation (2) (10^{-9} kg s^{-2})	Nominal sheath edge, equation (7) (mm)	Dust charge, equation (9) ($1000e$)
1.01 ± 0.02	6.67 ± 0.13	8.97 ± 0.01	125 ± 2	27.5 ± 0.9	0.065 ± 0.004	0.11 ± 0.01	9.6 ± 0.1	0.2 ± 0.1
1.52 ± 0.04	6.67 ± 0.13	9.17 ± 0.01	153 ± 2	8.5 ± 0.9	0.22 ± 0.02	0.52 ± 0.04	9.6 ± 0.1	0.8 ± 0.5
2.2 ± 0.1	6.67 ± 0.13	9.34 ± 0.01	192 ± 2	9.9 ± 0.9	0.67 ± 0.09	2.5 ± 0.3	9.6 ± 0.1	3.3 ± 2.1
3.46 ± 0.04	6.67 ± 0.13	8.93 ± 0.01	160 ± 2	5.1 ± 0.9	2.62 ± 0.09	6.7 ± 0.3	9.3 ± 0.1	4.8 ± 3.1
4.86 ± 0.03	6.67 ± 0.13	7.60 ± 0.01	85.7 ± 2	5.0 ± 0.9	7.2 ± 0.1	5.4 ± 0.3	8.9 ± 0.1	6.9 ± 4.1
6.85 ± 0.1	6.67 ± 0.13	6.95 ± 0.01	67.5 ± 2	3.5 ± 0.9	20.3 ± 0.9	9.3 ± 0.7	9.1 ± 0.2	18.6 ± 6.4
6.95 ± 0.1	6.67 ± 0.13	7.61 ± 0.01	69.0 ± 2	2.9 ± 0.9	21.2 ± 0.9	10.1 ± 0.7	9.7 ± 0.2	31.7 ± 9.9
1.01 ± 0.02	13.33 ± 0.13	8.68 ± 0.01	140 ± 2	51 ± 0.9	0.065 ± 0.004	0.14 ± 0.01	9.1 ± 0.1	0.3 ± 0.2
1.52 ± 0.04	13.33 ± 0.13	8.29 ± 0.01	138 ± 2	19 ± 0.9	0.22 ± 0.02	0.43 ± 0.04	8.8 ± 0.1	0.4 ± 0.2
2.2 ± 0.1	13.33 ± 0.13	8.65 ± 0.01	130 ± 2	24 ± 0.9	0.67 ± 0.09	1.2 ± 0.2	9.2 ± 0.1	3.7 ± 2.3
3.46 ± 0.04	13.33 ± 0.13	7.83 ± 0.01	74 ± 2	11 ± 0.9	2.62 ± 0.09	1.5 ± 0.1	9.6 ± 0.1	7.5 ± 3.3
4.86 ± 0.03	13.33 ± 0.13	7.84 ± 0.01	95 ± 2	11 ± 0.9	7.2 ± 0.1	6.6 ± 0.3	8.9 ± 0.1	12.9 ± 5.6
6.85 ± 0.1	13.33 ± 0.13	6.95 ± 0.01	59 ± 2	5.2 ± 0.9	20.3 ± 0.9	7.1 ± 0.6	9.7 ± 0.3	34.6 ± 9.6
6.95 ± 0.1	13.33 ± 0.13	6.58 ± 0.01	56 ± 2	5.4 ± 0.9	21.2 ± 0.9	$6.7 \pm .06$	9.7 ± 0.3	29.6 ± 9.3

20% of the sheath thickness. This amplitude range is much better than one would normally expect for a small-amplitude match between an arbitrary, non-parabolic potential well and a harmonic approximation. The close fits between theory and experiment over these large amplitude ranges tend to support our hypothesis that the electric potential is indeed very nearly harmonic throughout the sheath.

It is quite apparent that as the oscillation amplitude increases past a certain point, the quality of the fit drops markedly. This is due, in some part, to the fact that the trajectories of the higher-amplitude oscillations are not exclusively in the plasma sheath. While the dust continues to oscillate between the plasma and plasma sheath regions, the potential well it sees is not even approximately harmonic. As soon as the dust oscillations become damped enough to confine it exclusively to the sheath, the theoretical fit becomes much better. Another reason for the discrepancy between theory and experiment is our assumption of constant charge on the dust particle. The charging time of a dust particle has been shown to be on the order of 10^{-6} s [4, 19], much faster than our oscillation time scale of 10^{-2} s, so the dust charge might vary with position during an oscillation. The larger the oscillation, the worse our constant-charge assumption becomes, adding to the fit/data mismatch. Less massive dust particles, oscillating nearer the sheath edge, would seem to be affected more by both of these problems. They oscillate nearer the sheath edge where the harmonic potential assumption breaks down. They also have smaller charges, making even small charge changes during oscillations significant. These effects are apparent in figure 4, where the amplitude at which theory and experiment break down is much smaller for less massive particles.

As preliminary measures of agreement between theory and experiment, we compared our parameters with standard drag laws and the predicted sheath width from our harmonic theory. To determine the drag law on small spheres in a plasma sheath, we used our fitting parameter $(2\tau)^{-1}$ along with equation (3) to calculate the drag constant, γ. Our experimental results showed close (within 20%) agreement with the Epstein theory [15]. We next calculated the location of the minimum in the electrical potential energy from our experimentally determined restoring constants, κ, and equation (7). With a negative dust charge, this value would be where the maximum electrical potential would occur, or nominally, where the sheath edge should occur if the potential were globally harmonic. From this calculation (the results of which are presented in table 1), we obtained theoretical sheath widths of 9.5 ± 0.3 mm (6.67 Pa) and 9.2 ± 0.3 mm (13.33 Pa), agreeing quite well with our observed widths of 9.4 ± 0.25 and 8.5 ± 0.25 mm, respectively. Again, this agreement tends to support our assumption of a parabolic electric potential within the sheath

Equation (9) showed that determining the charge on a dust particle at its equilibrium position required a knowledge of not only its mass and the restoring constant, but also of the potential difference between two definite points in the sheath. Thus, we must develop a parabolic sheath potential function.

The first step in developing the potential function is to determine the potential drop across the driven sheath. To determine this drop, we assumed a two-sheath model $\phi_d = \phi_g + \phi_{sb}$, where ϕ_d and ϕ_g are the driven and grounded dc sheath potential differences and ϕ_{sb} is the measured dc self-bias between the grounded and driven electrodes. This model also requires that the sum of the ac sheath potentials, $\phi_{d,ac}$ and $\phi_{g,ac}$ equals the applied ac voltage, or $\phi_{d,ac} + \phi_{g,ac} = \phi_{ac}$. Calculation of the self-bias voltage developed across an RF-enhanced sheath was carried out using the standard method [26], for the case of zero dc current flow. We then iteratively solved for the dc sheath potential using these two equations.

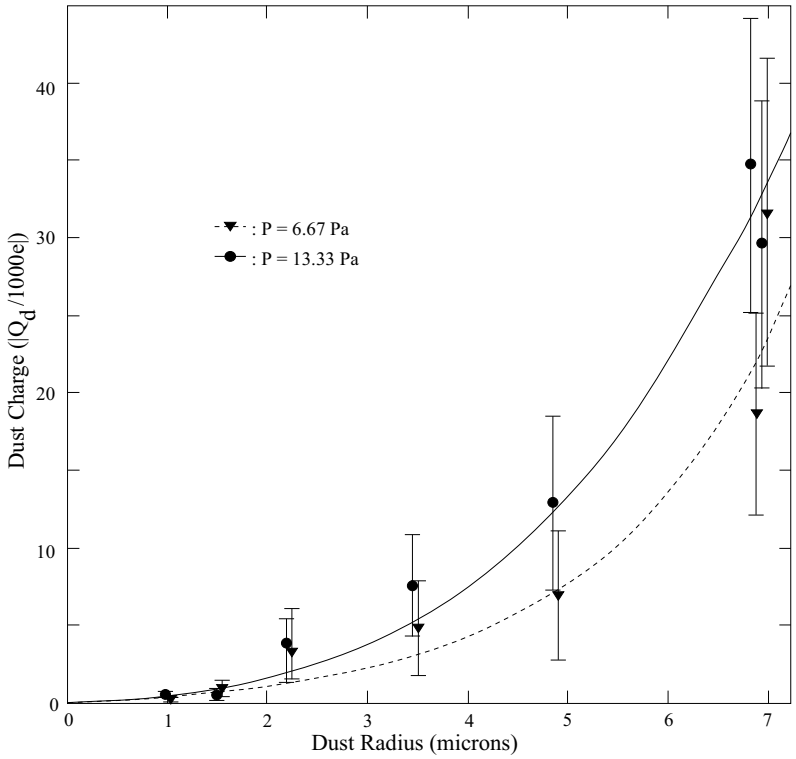

Figure 5. Variation of the dust charge as a function of dust radius. This figure shows plots of normalized dust charge for two different pressures: circles and the full curve represent the data and fit for $P = 13.33$ Pa while triangles and the broken curve show data and fit for $P = 6.67$ Pa. The circles are offset slightly to the left and the triangles to the right for clarity. The actual horizontal position is halfway between the pairs of error bars. The fits were obtained from equation (12), with the appropriate functions as noted in the text. This plot is for melamine formaldehyde suspended in an argon plasma.

In our experiment, the applied RF amplitude was 96.4 V and the self-biases were 56.9 ± 1.5 V (6.67 Pa) and 49.3 ± 1.9 V (13.33 Pa). Thus, the dc potentials across the driven electrode sheath were 86.3 ± 0.8 V (6.67 Pa) and 83.0 ± 1.0 V (13.33 Pa). The validity of this voltage division is supported by considering the resulting ratios of the effective areas of the grounded to driven electrodes [23, 27] of 1.7 (6.67 Pa) and 1.5 (13.33 Pa), ratios which are quite reasonable for our experimental set-up.

The boundary conditions for our parabolic sheath model then became: $\phi(0) = -86.3$ V, $z_{sh} = 9.4$ mm and $\phi(z_{sh}) = 0$ (6.67 Pa); and $\phi(0) = -83.0$ V, $z_{sh} = 8.5$ mm and $\phi(z_{sh}) = 0$ (13.33 Pa). The values for E_s come from equation (10). The potential functions derived from a parabolic fit to the above boundary conditions were $\phi(z) = -0.906(z - 9.77)^2 + 0.124$ (6.67 Pa) and $\phi(z) = -0.985(z - 9.21)^2 + 0.499$ (13.33 Pa), with z in millimetres and $\phi(z)$ in volts. We must emphasise that the potential functions presented here stem from what we consider to be the most reasonable choices of the boundary conditions from current literature. Should better parabolic boundary conditions be determined at a later date, they may be used with our data to provide improved results.

Once the potential functions had been determined, it was a relatively simple procedure to calculate the dust charge. These values for the dust charge are given in table 1, and are in reasonably good order of magnitude agreement with those of a number of previous researchers [3–6, 28], considering the differences in the experimental parameters.

The effect of changing the dust radius on the equilibrium charge is fairly complicated, as the increased radius not only provides a larger surface area, but also causes the dust to suspend lower in the sheath. To visualize this effect, we can rewrite equation (9) as a function of dust radius. Assuming a globally harmonic sheath potential, using the Epstein drag law ($\gamma = (1 + \pi/8)(4\pi/3)m_n\overline{u}_n n_n a^2$), substituting $(4\pi/3)a^3\rho$ for the dust mass, and employing equations (2), (3) and (9), we obtain the following equation for the charge as a function of dust radius:

$$Q_d(a) = \frac{2g^2\alpha^3 a^5}{K(z_{eq}(a) - z_0)^2[(2\alpha\omega(a)a)^2 + \beta^2]} \tag{12}$$

where

$$\alpha = \tfrac{4}{3}\pi\rho \tag{13}$$

and

$$\beta = \left(1 + \frac{\pi}{8}\right)\frac{4}{3}\pi m_n\overline{u}_n n_n \tag{14}$$

where, a is the sphere radius, n_n, m_n and $\overline{u}_n$ are the number density, mass and average speed of the neutral gas molecules, z_0 is the location of the maximum of the harmonic sheath electric potential, ρ is the mass density of the dust and K is the curvature of the modelled potential. Note that the constants α and β concern physical properties related to the dust particle and the suspending gas, respectively. The functional relationships $\omega(a)$ and $z_{eq}(a)$ must be determined from *experimental* results while the values for K and z_0 come from the *modelled* sheath potential.

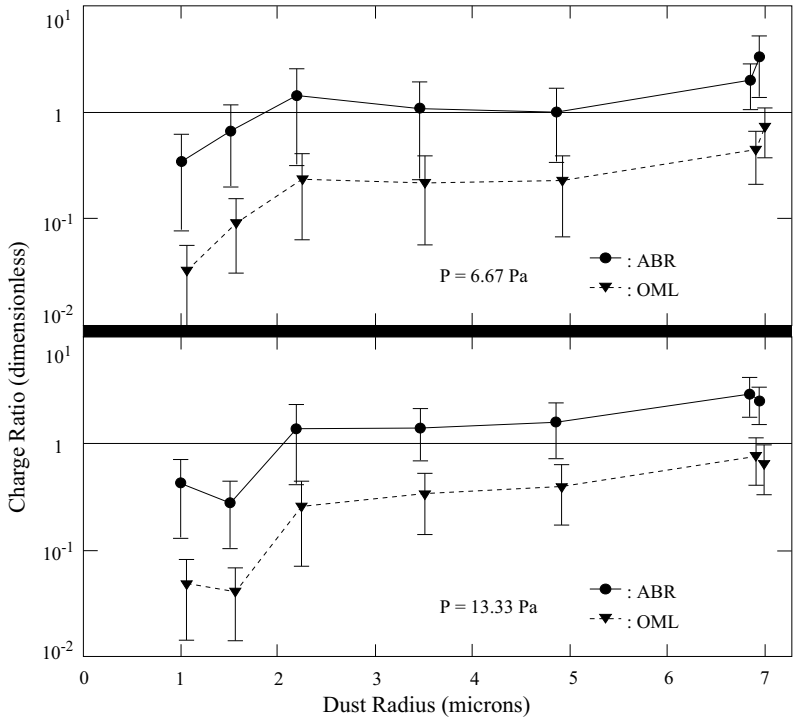

Figure 6. Comparison of dust charges from various theories. This plot shows the ratio of our experimental charge to the theoretical charge on spherical particles obtained from the radial (full lines and circles) and orbital motion limited (broken lines and triangles) theories. The upper and lower frames show the results for $P = 6.67$ Pa and $P = 13.33$ Pa, respectively. The circles are offset slightly to the left and the triangles to the right for clarity. The actual horizontal position is halfway between the pairs of error bars. The discrepancies between our measurements and the available theories are discussed in the text.

From the data listed in table 1, ω tended to be roughly quadratic in a, described approximately by the functions

$$\omega = 1.05 \times 10^{12} a^2 - 2.90 \times 10^7 \mathrm{a} + 2.21 \times 10^2 \qquad P = 6.67 \text{ Pa}$$

and

$$\omega = 1.31 \times 10^{12} \mathrm{a}^2 \ (\mathrm{s}^{-1}\ \mathrm{m}^{-2}) - 2.49 \times 10^7 \mathrm{a} \ (\mathrm{s}^{-1}\ \mathrm{m}^{-1}) + 1.68 \times 10^2 \ (\mathrm{s}^{-1}) \qquad P = 6.67 \text{ Pa}.$$

The linear relationship between z_{eq} and a was roughly described by $z_{eq} = -3.55 \times 10^2 \mathrm{a} + 9.73 \times 10^{-3}$ ($P = 6.67$ Pa) and $z_{eq} = -3.15 \times 10^2 a + 9.04 \times 10^{-3}$ ($P = 13.33$ Pa). In the above relationships, both z_{eq} and a are in metres and ω is in rad/s. Figure 5 shows the variation of dust charge against dust radius, along with the theoretical curve based on the above functions used in equation (12). The theoretical curve could be improved by using more complicated functional relationships for $\omega(a)$ and $z_{eq}(a)$. We chose to use the simple linear and quadratic relationships here to illustrate how a reasonably close fit could be made with very simple functional assumptions. The limited dependency of the charge of smaller particles on pressure has also been noted by other researchers [4].

To demonstrate that we can safely ignore the ion drag force on the smaller dust particles, let us assume that the worst case would be if the ion drag force were equal to the gravitational force on a 2.0 μm radius dust particle. (In reality, for this large a particle, the ion drag at the equilibrium height is about 20% of the magnitude of the gravitational force [19].) Our first approximation is to assume that this additional force causes the particle to suspend at the same height as a particle whose mass is twice as large, or whose radius is 2.5 μm. In this region of figure 5, the charge curve is very flat for both of the pressures shown. The change of the charge due to this change in radius, from equation (12), is just a noise-level 500 electron charges for the worst-case pressure (13.33 Pa).

We must emphasise that the assumptions that went into generating figure 5 are dependent upon the mass–density of the dust and the atomic mass of the suspending gas; this plot applies to melamine formaldehyde particles suspended in an argon plasma. The theory (equation (12)), however, may be adapted to any combination of dust and plasma gas.

7. Discussion

We attempted to compare our experimental charges with those obtained from purely theoretical work, but a self-consistent theory of particulate charging in the *plasma sheath* does not appear to exist. (At least two sheath-charging models [19, 29] have been developed. However, they both rely on the orbital motion limited (OML) charging theory, e.g. [30], which does not seem to be a good approximation in the non-central field environment surrounding dust particles in the plasma sheath.) Several theories concerning dust charging in a *plasma* environment exist, and we investigated the correlation of our results with some of those theories.

Nairn *et al* [16] published a charging theory that numerically calculates floating potentials for spherical particles in a plasma based on the Allen, Boyd and Reynolds

(ABR) radial motion theory [31] of the ions toward the particle. The charge on the particle may then be calculated using the vacuum capacitance equation

$$Q_d = 4\pi\varepsilon_0 a V_f \tag{15}$$

where ε_0 is the permittivity of free space and V_f is the floating potential, valid in the small a/λ_D limit. (Equation (15) has been shown to be valid for our case of small, isolated spheres surrounded by screening charges, as is the case in the sheath [32].) In this theory, the floating potential approaches a non-zero constant as the ratio a/λ_D becomes small. Improved numerical techniques [33] have shown that the floating potential should actually approach zero as that ratio approaches zero. Nairn has also calculated the floating potentials that arise due to the widely quoted OML theory. We present results based on this theory as well, although the general validity of OML is being seriously questioned [34]. We also note that the charges calculated in much of the previous work [3–5, 7] rely on the OML charging theory.

We have calculated the theoretical charges on dust particles having the same a/λ_D ratios as our experimental data. The ratios of our experimental charges to the theoretical charges from the radial motion and OML theories are shown in figure 6. It is obvious from figure 6 that our experimental charges do not agree with the questionable OML charging theory. We find somewhat better agreement with charging calculations based on the ABR (radial motion) theory. It should be remembered, however, that the ABR theory was originally developed for a probe in a quasineutral plasma, not in the space-charge sheath region. We present these results primarily as a motivation for the development of an applicable charging theory in the sheath.

We also note that the charges presented in this paper most likely are slight underestimates. When we use the potential from our model in equation (9), we tacitly assumed that only the charge on the dust is the charge responsible for the oscillation characteristics. In reality, the dust floats at a potential somewhat lower than the local potential [19]. Dust particles attract a sheath of screening ions that moves with the dust throughout its oscillations (individual ions do not remain with the dust, but collectively, the total screen does). The charge of this moving screen will affect the oscillation parameters, and hence the calculated charge. Another way of looking at this effect is to note that as ions are deflected by the negative potential of the dust particle, they form a region of higher ion concentration below the particle. Calculations of this effect in a plasma (not the sheath) were carried out by Stangeby and Allen [35]. The electrostatic attraction between this positive ion wake region and the negatively charged dust particle (and repulsion between the wake and the shielding ions) could cause variations in the equilibrium height, inducing charge calculation errors. Quantitative estimates of this effect require the development of a theory of charging in the sheath.

8. Summary

We have made a number of assumptions to produce the results in this work. For our theory, we assume that the total potential energy is globally harmonic and that the charge on the dust particle remains constant during the oscillation. These assumptions imply that the electric potential must also be harmonic.

We have shown that our experimental results strongly support the assumption that the potential in the plasma sheath is generally parabolic. Our harmonic oscillation theory alone leads to results that agree quite well with the established drag laws. Our parabolic model of the sheath potential, while extremely simple, agrees well with numerical models of much higher complexity. Those models also predict parabolic time-averaged sheath potentials, again supporting our original harmonic assumption. The large amplitude ranges over which the dust oscillation trajectories fit the damped harmonic oscillator theory also tend to support the existence of a harmonic sheath potential. When we combine the harmonic oscillation theory with our simplified sheath model, we are able to deduce the charge on dust particles suspended in the sheath.

Acknowledgments

We express our appreciation to the United Kingdom Engineering and Physical Sciences Research Council (EPSRC) for their financial and material support of this project. The loan of the high-speed camera from the EPSRC equipment pool is gratefully acknowledged. One of us (EBT) would also like to thank the United States Air Force for supporting his research. This research was greatly facilitated by custom video analysis software developed by D A Law and the many useful discussions with Dr Law and W H Steel.

References

[1] Chu J H, Du J B and Lin I 1994 *J. Phys. D: Appl. Phys.* **27** 296
[2] Thomas H, Morfill G E, Demmel V, Goree J, Feuerbacher B and Mohlmann D 1994 *Phys. Rev. Lett.* **73** 652
[3] Melzer A, Trottenberg T and Piel A 1994 *Phys. Lett.* A **191** 301
[4] Trottenberg T, Melzer A and Piel A 1995 *Plasma Sources Sci. Technol.* **4** 450
[5] Kortshagen U and Mümken G 1996 *Phys. Lett.* A **217** 126
[6] Homann A, Melzer A and Piel A 1999 *Phys. Rev.* E **59** R3835
[7] Nunomura S, Misawa T, Ohno N and Takamura S 1999 *Phys. Rev. Lett.* **83** 1970
[8] Konopka U, Ratke L and Thomas H M 1997 *Phys. Rev. Lett.* **79** 1269
[9] Morfill G E, Thomas H M, Konopka U and Zuzic M 1999 *Phys. Plasmas* **6** 1769
[10] Tomme E B, Law D A, Steel W H, Annaratone B M and Allen J E 1998 *Proc. 14th European Conf. Atomic and Molecular Physics Ionised Gases (ESCAMPIG) (Malahide, Ireland)* Europhysics Conference Abstracts vol 22H, p 334
[11] Northrop T G and Birmingham T J 1990 *Planet. Space Sci.* **38** 319
[12] Barnes M S, Keller J H, Forster J C, O'Neill J A and Coultas D K 1992 *Phys. Rev. Lett.* **68** 313
[13] Kilgore M D, Daugherty J E, Proteous R K and Graves D B 1993 *J. Appl. Phys.* **73** 1617
[14] Baerline R 1983 *Newtonian Dynamics* (London: McGraw-Hill) pp 45–70
[15] Epstein P S 1924 *Phys. Rev.* **23** 710

[16] Nairn C, Annaratone B M and Allen J E 1998 *Plasma Sources Sci. Technol.* **7** 478
[17] Blank J L 1968 *Phys. Fluids* **11** 1686
[18] Skorik M and Allen J E 1993 *Proc. 21st Int. Conf. Phenomena in Ionized Gases (Bochum, Germany)* p 113
[19] Nitter T 1996 *Plasma Sources Sci. Technol.* **5** 93
[20] Franklin R N and Snell J 1997 *J. Phys. D: Appl. Phys.* **30** L45
[21] Riemann K-U 1991 *J. Phys. D: Appl. Phys.* **24** 493
[22] Riemann K-U 1997 *Phys. Plasmas* **4** 4158
[23] Salem M M and Loiseau J F 1996 *J. Phys. D: Appl. Phys.* **29** 1181
[24] Nitter T, Aslaksen T K, Melandsø F and Havnes O 1994 *IEEE Trans. Plasma Sci.* **22** 159
[25] Melandsø F 1992 *Phys. Scr.* **45** 515
[26] Boschi A and Magistrelli F 1963 *Nuovo Cimento* **29** 487
[27] Maniv S 1988 *J. Appl. Phys.* **63** 1022
[28] Law D A, Tomme E B, Steel W H, Annaratone B M and Allen J E 1999 *Proc. 24th Int. Conf. Phenomena in Ionized Gases (Warsaw, Poland)* **4** 109
[29] Chen X 1997 *IEEE Trans. Plasma Sci.* **25** 1117
[30] Allen J E 1992 *Phys. Scr.* **45** 497
[31] Allen J E, Boyd R L F and Reynolds P 1957 *Proc. Phys. Soc.* B **70** 297
[32] Whipple E C, Northrop T G and Mendis D A 1985 *J. Geophys. Res.* **90** 7405
[33] Kennedy R 1999 *Proc. 24th Int. Conf. Phenomena in Ionized Gases (Warsaw, Poland)* **3** 97
[34] Allen J E, Annaratone B M and de Angelis U 2000 *J. Plasma Phys.* **63** 299
[35] Stangeby P C and Allen J E 1971 *J. Plasma Phys* **6** 19